Proceedings of the 28th IEEE
EMBS Annual International Conference
New York City, USA, Aug 30-Sept 3, 2006

Very Low Frequency Modulation in Renal Autoregulation

Kin L. Siu[1], Biin Sung[1], Leon C. Moore[2], Aija Birzgalis[2] and Ki H. Chon[1], *Member, IEEE*

[1]Biomedical Engineering, [2]Physiology and Biophysics, SUNY at Stony Brook, HSC T-18 Rm 30, Stony Brook, NY, 11794

Abstract—**This study aims to examine the presence of a possible third renal autoregulatory mechanism in the very low frequency (VLF) band (~10 mHz) using a high-resolution time-frequency spectral method. Blood pressure and renal blood flow data were measured from conscious and anesthetized Sprague-Dawley and spontaneously hypertensive rats, at the level of the whole kidney (via ultrasound flow probe) and local cortical tissue of a kidney (via laser Doppler flow probe). In addition, N-nitro-L-arginine (LNAME) was used in order to assess the effect of nitric oxide on the third mechanism. Using a complex demodulation method with high time and frequency resolution, a VLF band was often observed, as well as amplitude modulation at the VLF of the two other autoregulation mechanisms. The presence of amplitude modulation is an indication of a particular form of nonlinear interaction between the autoregulatory mechanisms. Physically, such interactions may arise from the fact that all three mechanisms share a common effector, the afferent arteriole. In addition, the magnitude of amplitude modulation of the VLF on the other autoregulatory mechanisms was enhanced by the addition of LNAME, suggesting an important role of nitric oxide in the autoregulatory process.**

I. Introduction

Arterial blood pressure varies spontaneously over many time scales and on the order of 50% of the mean value [1]. These fluctuations threaten to overwhelm renal excretory function, but changes in glomerular filtration rate and solute excretion are minimized by mechanisms responsible for providing autoregulation of renal blood flow. Furthermore, recent evidence suggests that autoregulation may also function to protect the renal vasculature from sudden changes in systemic pressure [2]. Moreover, susceptibility to renal injury in hypertension and the progression of chronic renal failure is exacerbated by autoregulatory dysfunction [3]. Hence, it is important to characterize the dynamic features of renal autoregulatory mechanisms and their differences between normal and diseased states.

Renal autoregulation is mediated by the tubuloglomerular feedback (TGF) and the myogenic (MYO) mechanisms, with resonant frequencies at 0.02-0.05 and 0.1-0.3Hz, respectively [4]. Recently, Just and Arendshorst [5] suggested the possibility of an existence of a third renal autoregulatory mechanism with a time constant of ~100 sec. In their study, the steady state analysis of time-domain characteristics of the third mechanism was investigated, but its dynamic characteristics have not yet been investigated.

The dynamic properties of a biological system can normally be efficiently characterized by using time-frequency analysis techniques [6]. However, due to the operating time scale of the third mechanism (~0.01Hz), it is difficult to resolve its dynamics even with high resolution-time-frequency spectral methods. A further complication is that frequency of the third mechanism is close to the operating range of the TGF mechanism. Therefore, to accurately resolve the third mechanism, one must use either long data sets or a more sophisticated technique to detect the presence of the very low frequency oscillation.

Recently, we have reported the presence of nonlinear interactions between the TGF and MYO mechanisms [7, 8]. If the third mechanism does indeed exist, then it is possible that the nonlinear interactions between these two mechanisms with the third mechanism may also exist. The presence of the amplitude and frequency modulations are indication of a particular form of nonlinear interaction between these hemodynamic control systems.

In this paper, the aim is to determine if the third mechanism interacts with the other two renal autoregulatory mechanisms by identifying amplitude and frequency modulation using a high-resolution time-frequency method based on complex demodulation (CDM) [9]. To examine if interactions occur among three autoregulatory mechanisms, records of systemic blood pressure and renal blood flow were obtained. Renal blood flow was measured at the level of the whole kidney or in renal cortical tissue in Sprague-Dawley (SDR) and spontaneously hypertensive rats (SHR), in both conscious and anesthetized conditions. Further, N-nitro-L-arginine (LNAME) was used to assess the effect of nitric oxide (NO) on the third mechanism, as it has been reported that LNAME accentuates amplitude modulation of renal blood flow fluctuations [10].

II. Methods

A. Animal Model

All experiments were conducted on male SDR and SHR between 190-230g in accordance with the institutional guidelines for the care and use of research animals. The animals had free access to food and water prior to experiments.

For telemetry experiments (n = 3: SDR, n = 2: SHR), animals were anesthetized using pentobarbital sodium

This research was supported by NIH HL69629

(50mg/kg, i.p.). An incision was made on the left flank. The left renal artery was isolated and cleared of connective tissue. An ultrasound probe (Transonic, Ithaca, NY) was implanted onto the left renal artery. The connector end of the probe was fed under the skin to the back of the animal between the shoulder blades to avoid damage by the animal. The left flank was then stitched back together. The left femoral artery was then catheterized and connected to a telemetric blood pressure sensor (Data Science International, Arden Hills, MN). After the surgery, animals were allowed 1 week to recover before the start of data collection.

For acute experiments, animals were anesthetized using Inactin (n = 5: SDR; n = 3: SHR) (Sigma) or Isoflurane (n = 4:SDR; n = 2: SHR) (Baxter) at 135mg/kg i.p. and ~1 percent inspired gas, respectively. Animals were then placed on a temperature-controlled surgery table to maintain the body temperature at 37°C. The tracheostomy was performed on the animal (PE240 tubing) to allow for unobstructed breathing. For isoflurane anesthetized animals, the tracheostomy tube was connected to a respirator (50/50 oxygen/nitrogen, ~70 beats per minute). The left femoral artery and vein were catheterized (PE-50 and PE-10 tubing) to allow for measurement of arterial pressure and continuous infusion of saline, respectively. The left kidney was isolated and place in a Lucite cup and the cortical surface was covered with a thin plastic film to prevent fluid evaporation. Cortical blood flow was measured via a blunt 11-gauge needle laser-Doppler probe (Transonic, Ithaca, NY) place on the cortical surface. Whole kidney blood flow was measured via an ultrasound flow probe (Transonic, Ithaca, NY) placed around the renal artery. A surgical lubricant, Surgilube® (E. Fougera & CO., Melville, NY), was applied around the flow probe to ensure proper conduction of ultrasound signal. Renal perfusion pressure was controlled with a suprarenal aortic clamp.

B. Data Collection

For telemetry animals, data were collected for 1-2 hours per day. All animals were observed during the data collection period for their activity. Due to motion artifacts, only the portions of data where animals remained relatively calm were used. After one week of baseline measurements, LNAME was introduced into the drinking water (25mg/kg/day). Raw data were collected at a sampling rate of 250 Hz. The data were down-sampled to 1Hz after low-pass filtering to avoid aliasing.

For acute animals, spontaneous baseline data were collected for 30 minutes. To induce full activation of autoregulatory mechanisms' dynamics a mechanical clamp was placed on the suprarenal aortic artery which was used to rapidly reduce blood pressure by ~20-30mmHg. After stabilization of renal blood flow following tightening of the clamp, the clamp was rapidly released and the resultant transient blood flow data were measured. Following a series of clamp trials, L-NAME was infused at a continuous rate. After blood pressure and blood flow stabilization, spontaneous data measurements were collected for approximately 30 minutes followed by the use of a clamp to fully elicit dynamics of the autoregulatory mechanisms. Data were collected at a sampling rate of 100Hz. The analyzed data were down-sampled to 1Hz after low-pass filtering to avoid aliasing. All data including acute and telemetry recordings were normalized to zero mean and unit variance.

C. Complex Demodulation Method

The complex demodulation method is described in detail in [9] and thus, will only be briefly summarized.

Consider a sinusoidal signal $x(t)$ to be a narrow band oscillation with a center frequency f_0, instantaneous amplitude of $A(t)$, phase $\Phi(t)$, and the direct current component $dc(t)$:

$$x(t) = dc(t) + A(t)\cos(2\pi f_0 t + \phi(t)) \tag{1}$$

Multiplying Eq. 1 by $e^{-j2\pi f_0 t}$ provides:

$$z(t) = x(t)e^{-j2\pi f_0 t} = dc(t)e^{-j2\pi f_0 t} + \frac{A(t)}{2}e^{j\phi(t)} + \frac{A(t)}{2}e^{-j(4\pi f_0 t + \phi(t))} \tag{2}$$

If $z(t)$ in Eq. (2) is filtered by an ideal low-pass filter with a cutoff frequency of $f_c < f_0$, the filtered signal $z_{lp}(t)$ will contain the following:

$$z_{lp}(t) = \frac{A(t)}{2}e^{j\phi(t)}$$
$$A(t) = 2\left|z_{lp}(t)\right| \tag{3}$$
$$\phi(t) = \arctan\left(\frac{imag(z_{lp}(t))}{real(z_{lp}(t))}\right)$$

We consider a case when a modulating frequency is not fixed as described above but varies as a function of time. In this case the signal $x(t)$ can be written in the following form:

$$x(t) = \sum_i d_i = dc(t) + \sum_i A_i(t)\cos\left(\int_0^t 2\pi f_i(\tau)d\tau + \phi_i(t)\right) \tag{4}$$

Using the Hilbert transform, the instantaneous amplitude and frequency of d_i can be obtained. The entire time-frequency spectrum (TFS) can be obtained by the calculation of the Hilbert transform of Eq. (4) for all time points for the obtained low-pass filtered frequency components, as described in Eq. (3).

D. Amplitude Modulation Detection: Simulation Example

Using the TFS estimated from the above-described CDM method, the average amplitude and the peak frequency in the TGF and MYO frequency bands (0.02-0.05 Hz and 0.1-0.3 Hz, respectively) were extracted at each time instant. To determine the frequencies associated with these extracted

amplitude and frequency oscillations, power spectral densities (PSD) were subsequently calculated. To quantitatively determine if the spectral power of the amplitude oscillations were statistically significant, 100 independent time series consisting of 0 dB and 20 dB Gaussian white noise (GWN) were generated. Each of these 100 0 dB and 20 dB GWN time series were processed in the same manner as the simulated or measured experimental data. The mean plus two standard deviations of the PSD of the 100 GWN time series was used as the statistical thresholds for 0 dB and 20 dB noise. Spectral power above these statistical thresholds indicates 95% probability that the frequency or amplitude modulation cannot be explained by some random occurrence. Fig. 1 shows an example of the amplitude modulation (AM) detection on a simulated signal composed of two sinusoids (HF = 0.2 Hz and LF = 0.03 Hz) modulated by a slower frequency (VLF = 0.01Hz). Superimposed on Fig. 1 are dotted lines to represent the statistical threshold based on 0 dB GWN. The fact that these statistical lines are below the spectral peaks associated with the AM illustrates that this method is able to detect VLF interaction with two higher frequency oscillators.

III. Results

Fig. 2 shows a typical renal blood flow data obtained at two different kidney levels of measurements. Also shown are the amplitude and frequency modulation spectra, and the statistical threshold spectra. Figs. 3-4 shows the magnitude of the spectra obtained from the AM associated with the MYO (figure 3) and TGF (figure 4). Further, Figs. 3-4 shows the effect of LNAME on the modulation magnitudes.

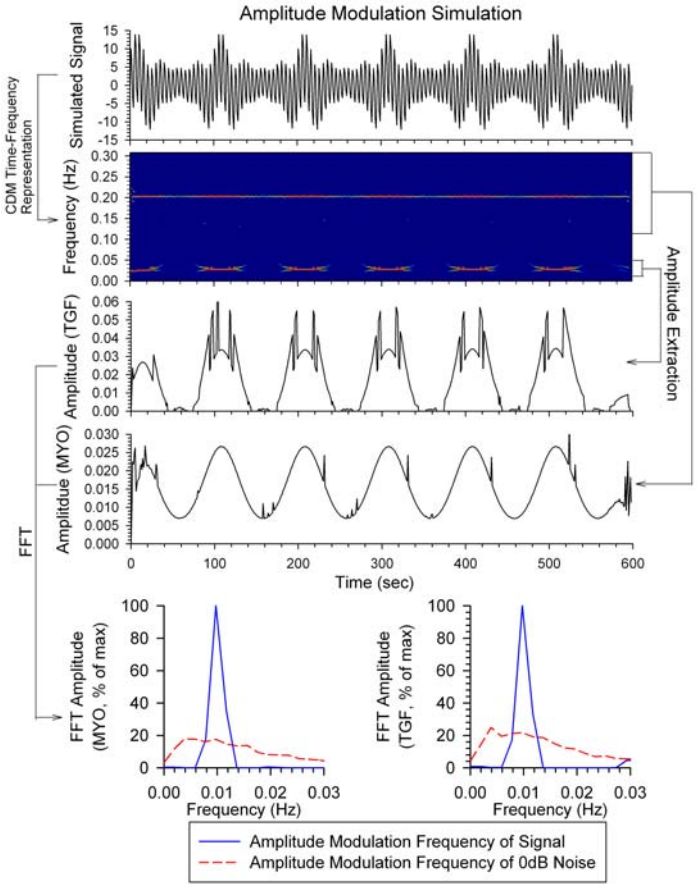

Figure 1 – Extraction of amplitude modulation from a simulated signal. The simulated signal contains two frequencies (0.03 and 0.2Hz) modulated by a low frequency (0.01Hz).

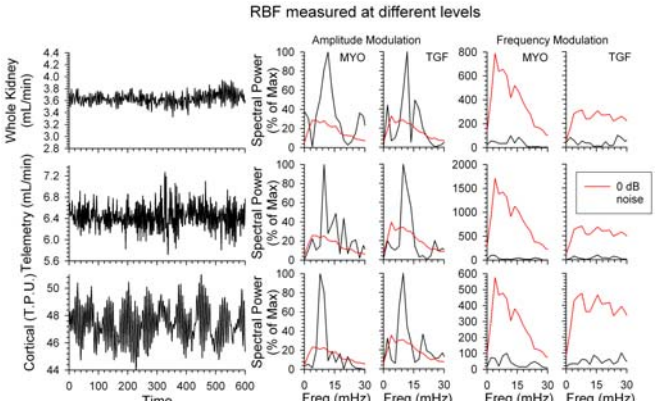

Figure 2 – Typical renal blood flow traces measured in SDR at the level of the whole kidney (anesthetized and conscious, top and middle respectively), and local cortical tissue (bottom). Amplitude and frequency modulation spectrum is also shown on the right.

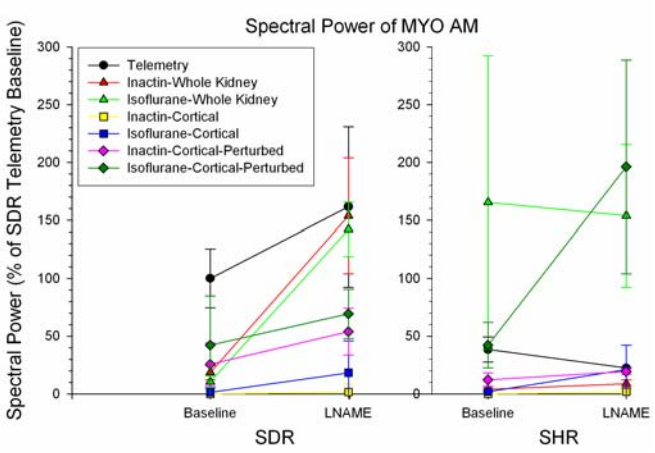

Fig. 3 – Amplitude modulation power extracted from the MYO frequency band under different conditions, both before and after the administration of L-NAME

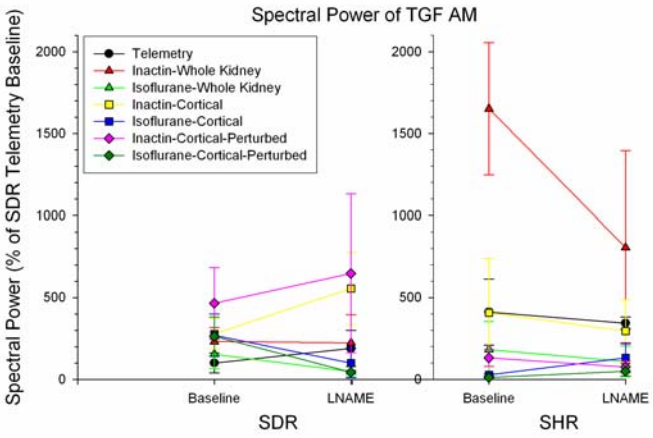

Fig. 4 – Amplitude modulation power extracted from the TGF frequency band under different conditions, both before and after the administration of L-NAME

IV. Discussion

In this paper, we show that it is possible to identify a very low frequency component in renal blood flow records, which may represent the putative third renal autoregulatory mechanism. This was done by analyzing amplitude and frequency modulation of the oscillations of the TGF and MYO systems by the VLF mechanism. As shown in Fig. 2, the spectral peak for amplitude modulation of both MYO and TGF oscillations by the VLF, centered at 0.01 Hz, was significantly higher than the 0dB statistical noise threshold for all baseline measurements in SDR, but not in SHR (not shown). However, with a 20 dB white noise threshold, the amplitude modulation of the VLF on both MYO and TGF were statistically significant for both strains of rats. However, this method was unable to detect significant frequency modulation by the VLF component in either rat strain and at both noise levels (see right panels of Fig. 2).

The presence of the statistically significant amplitude modulation peaks in RBF measurements suggests 1) that a very low frequency component is present and 2) that it interacts nonlinearly with the other autoregulatory mechanisms. Traditional time-invariant spectral analysis methods are incapable of detecting such amplitude modulation which are both nonlinear and nonstationary, whereas high-resolution CDM-based time-frequency approaches can resolve VLF amplitude modulation.

Infusion of LNAME tends to amplify the AM peak associated with MYO, while its effect on TGF is more anesthetic dependent. For Inactin-anesthetized animals, the VLF amplitude modulation spectral peak associated with TGF increased with LNAME, while this spectral peak decreased when isoflurane anesthetic was used. The important finding is that the addition of LNAME changes the characteristics of the amplitude modulation, and that nitric oxide may be responsible for the alteration.

As shown in Figs. 3 and 4, the magnitude of amplitude modulation varies with the strain of rat, choice of anesthetic, and the location of renal blood flow measurements. In general, the magnitude of the spectral peak of amplitude modulation on MYO is higher in the whole kidney than in the cortical tissue. In addition, isoflurane-anesthetized animals tend to have stronger amplitude modulation of the MYO oscillation than in Inactin-anesthetized animals. For TGF, amplitude modulation was stronger with Inactin anesthesia.

Although the amplitude modulation of the very low frequency on the TGF and MYO mechanisms detected in our study has the same time constants as reported by Just and Arendhorst [5], it is unclear whether both phenomena arise from a single source. Further experiments are needed to clarify this issue.

V. References

[1] D. J. Marsh, J. L. Osborn, and A. W. Cowley, Jr., "1/f fluctuations in arterial pressure and regulation of renal blood flow in dogs," *Am J Physiol*, vol. 258, pp. F1394-400, 1990.

[2] R. Loutzenhiser, K. A. Griffin, and A. K. Bidani, "Systolic blood pressure as the trigger for the renal myogenic response: protective or autoregulatory?," *Curr Opin Nephrol Hypertens*, vol. 15, pp. 41-9, 2006.

[3] A. K. Bidani, M. M. Schwartz, and E. J. Lewis, "Renal autoregulation and vulnerability to hypertensive injury in remnant kidney," *Am J Physiol*, vol. 252, pp. F1003-10, 1987.

[4] K. P. Yip, N. H. Holstein-Rathlou, and D. J. Marsh, "Dynamics of TGF-initiated nephron-nephron interactions in normotensive rats and SHR," *Am J Physiol*, vol. 262, pp. F980-8, 1992.

[5] A. Just and W. J. Arendshorst, "Nitric oxide blunts myogenic autoregulation in rat renal but not skeletal muscle circulation via tubuloglomerular feedback," *J Physiol*, vol. 569, pp. 959-74, 2005.

[6] R. Zou, W. A. Cupples, K. P. Yip, N. H. Holstein-Rathlou, and K. H. Chon, "Time-varying properties of renal autoregulatory mechanisms," *IEEE Trans Biomed Eng*, vol. 49, pp. 1112-20, 2002.

[7] K. H. Chon, Y. M. Chen, V. Z. Marmarelis, D. J. Marsh, and N. H. Holstein-Rathlou, "Detection of interactions between myogenic and TGF mechanisms using nonlinear analysis," *Am J Physiol*, vol. 267, pp. F160-73, 1994.

[8] K. H. Chon, R. Raghavan, Y. M. Chen, D. J. Marsh, and K. P. Yip, "Interactions of TGF-dependent and myogenic oscillations in tubular pressure," *Am J Physiol Renal Physiol*, vol. 288, pp. F298-307, 2005.

[9] H. Wang, K. Siu, K. Ju, and K. H. Chon, "A high resolution approach to estimating time-frequency spectra and their amplitudes," *Ann Biomed Eng*, vol. 34, pp. 326-38, 2006.

[10] Y. Shi, X. Wang, K. H. Chon, and W. A. Cupples, "Tubuloglomerular feedback-dependent modulation of renal myogenic autoregulation by nitric oxide," *Am J Physiol Regul Integr Comp Physiol*, vol. 290, pp. R982-91, 2006.